A Variable Speed Synchronous Motor Approach for Smart Irrigation using Doubly Fed Induction Motor

Un enfoque de motor síncrono de velocidad variable para el riego inteligente utilizando un motor de inducción doblemente alimentado

DOI: http://doi.org/10.17981/ingecuc.19.2.2023.02

Scientific Research Article. Date of Reception: 29/02/2023. Date of Acceptance: 27/03/2023.

Emad Hassan
Jazan University. Jizan (Saudi Arabia)
eshassan@jazanu.edu.sa

Ahmed S. Oshaba
Jazan University. Jizan (Saudi Arabia)
aoshaba@jazanu.edu.sa

Dina S. M. Osheba
Menoufiya University. Shibin El-kom (Egypt)
engdina20085@yahoo.com

Mervet A. Shanab
Menoufiya University. Shibin El-kom (Egypt)
mirvat.shanab@sh-eng.menofia.edu.eg

To cite this paper
E. Hassan, A. Oshaba, D. Osheba & M. Shanab, "A Variable Speed Synchronous Motor Approach for Smart Irrigation using Doubly Fed Induction Motor", *INGE CUC*, vol. 19, no. 2, pp. 21–32, 2023. DOI: http://doi.org/10.17981/ingecuc.19.2.2023.02

Abstract

Introduction— Doubly Fed Induction Motor (DFIM) is a popular machine used in variable speed drives, and its ruggedness, reliability and simplicity of speed control make it a suitable candidate for use in smart irrigation systems.

Objective— This paper studies and evaluates the performance of DFIM at different operating conditions and shows that it can be viewed as a variable speed synchronous motor.

Methodology— A mathematical model has been developed to optimize the performance of the DFIM in smart irrigation systems, taking into account the specific conditions of the application. In addition, an experimental setup was built and tested to enhance the theoretical results, which showed good correlation between the theoretical and experimental results.

Results— The research results reveal that DFIM can be used to control the flow rate of water in irrigation systems, by adjusting the speed of the motor to match the desired flow rate.

Conclusions— The results of this research demonstrate the potential of using the DFIM in smart irrigation systems to improve the performance and efficiency of irrigation and to provide better control and lower costs.

Keywords— Doubly Fed Induction Motor; Synchronous Motor; smart irrigation; Steady State Performance

Resumen

Introducción— El Motor de Inducción de Doble Alimentación (DFIM) es una máquina muy utilizada en accionamientos de velocidad variable, y su robustez, fiabilidad y sencillez de control de velocidad lo convierten en un candidato idóneo para su uso en sistemas de riego inteligente.

Objectivo— En este trabajo se estudia y evalúa el rendimiento del DFIM en diferentes condiciones de funcionamiento y se demuestra que puede considerarse como un motor síncrono de velocidad variable.

Methodología— Se ha desarrollado un modelo matemático para optimizar el rendimiento del DFIM en sistemas de riego inteligentes, teniendo en cuenta las condiciones específicas de la aplicación. Además, se construyó y probó un montaje experimental para mejorar los resultados teóricos, que mostró una buena correlación entre los resultados teóricos y experimentales.

Resultados— Los resultados de la investigación revelan que el DFIM puede utilizarse para controlar el caudal de agua en sistemas de riego, ajustando la velocidad del motor para que coincida con el caudal deseado.

Conclusiones— Los resultados de esta investigación demuestran el potencial del uso del DFIM en sistemas de riego inteligentes para mejorar el rendimiento y la eficiencia del riego y proporcionar un mejor control y menores costes.

Palabras clave— Motor de inducción doblemente alimentado; motor síncrono; riego inteligente; rendimiento en estado estacionario

I. Introduction

Doubly Fed Induction Motor (DFIM) looks a promising solution for variable speed drives. The lower capacity of the frequency converter handled in the rotor, achieves a significant cost saving compared to the systems that uses a full power converter. DFIM is mainly a wound rotor induction motor whose its rotor is supplied from a variable frequency converter. It is widely used as a generator for wind energy conversion systems owing to the constant frequency of the generated voltage obtained in spite of the rotor speed variation. In addition, the rotor speed can be controlled to obtain the maximum power from the wind turbine. DFIM also finds its application in electric and hybrid electric vehicles [1], [2], marine propulsion [3], [4], pumping systems [5], [6], and traction [7].

The steady state performance of DFIM have been investigated in several studies [7], [8], [9]. The speed variation of DFIM is performed based on changing the injected rotor voltage. Also, the results demonstrated that the DFIM's torque-speed characteristics are identical to those induction motor. Through theoretical studies, the steady-state operation of the DFIM has also been studied [10]. In this paper, the stator is excited at the supply frequency while the rotor is supplied by a voltage of frequency differs from the slip frequency. As a result, the machine operation is not stable and higher torque pulsations are obtained.

Recently, DFIM speed control is achieved via different control strategies. The field-oriented control of DFIM based on rotor position sensorless operation has been presented in ALGR, PL and UK research [11], [12], [13]. A single frequency converter is employed in the rotor side while the stator side is directly connected to the grid. Throughout KR, the sensor less field oriented control of DFIM is also studied but with two converters are employed [14], one in the stator side and the other in the rotor side. This is to perform the field orientation in both the stator and rotor. However, this increases the system cost and complexity. Direct torque control of DFIM has been studied as in CN, IR and IN [15], [16], [17]. This method of control achieves the direct and independent control of the motor torque and flux depending on the space vector modulation technique. Recently, fuzzy logic controller has been employed in direct torque control as an alternative to PI controller in order to eliminate the torque and flux ripples [18]. Sliding mode control is a novel control strategy of DFIM speed control [19]. It is an adaptive control scheme which achieves a robust performance of the motor drive despite the parameters' variation. All the recent papers reveal that the performance of DFIM resembles the conventional induction motor. The main contributions of this paper can be summarized as follows:

1) This paper studies the performance characteristics of DFIM under speed and load variation.
2) The mathematical model for DFIM in smart irrigation systems, is developed and implemented to predict the machine performance at different operating conditions.
3) Finally, an experimental setup was built and tested to enhance the theoretical results, which showed good correlation between the theoretical and experimental results.

II. System Description and Principle of Operation

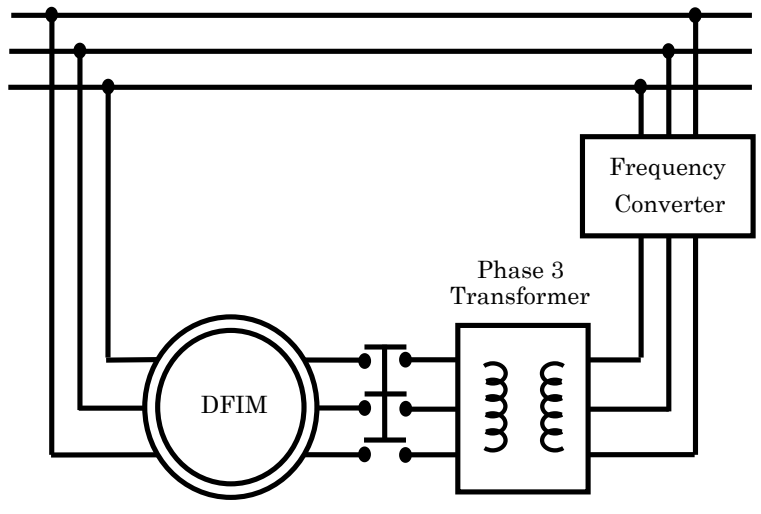

Fig. 1. A schematic diagram of DFIM drive system.
Source: Authors.

Fig. 1 depicts a schematic diagram of DFIM drive system. The stator three-phase terminals are supplied directly from the main supply, while the rotor windings are connected to the grid via a variable frequency converter. A three phase transformer is employed after the converter to reduce the output voltage from the converter to be suitable for the rotor windings.

The stator windings of DFIM are excited by the three phase ac currents from the grid, a rotating field is established in the stator. In other words, a rotating field is also created in the rotor windings as they are fed from the grid via the frequency converter. The interaction between the two rotating fields results in the motor rotating. Accordingly, the speed and direction of both the two rotating fields are the main parameters that control the motor speed. When both magnetic fields rotate in the same direction, the rotor will rotate at a speed equal to the difference between the speeds of the two rotating fields. Hence, the motor speed will be less than the synchronous speed. On the other hand, when both magnetic fields rotate in opposite direction, the rotor will rotate with a speed equal to the sum of the speeds of the two magnetic fields; consequently, the motor speed will be greater than the synchronous speed. This can be described by (1):

$$N_r = N_{s1} \pm N_{s2} = \frac{60(F_1 \pm F_2)}{P} \tag{1}$$

Where N_r is the motor speed in (rpm), N_{s1} is the rotating magnetic field speed in the stator in (rpm), and N_{s2} is the rotating magnetic field speed in the rotor in (rpm). F_1 represents the frequency of the AC currents fed into the stator windings, while F_2 represents the frequency of the AC currents fed into the rotor windings, and P is the number of pair poles of DFIM.

III. Mathematical Analysis

The steady-state mathematical model of DFIM is derived from the fundamental principles of induction motor as described by Indian studies [20]. The equivalent circuit per phase of wound rotor induction motor in case of feeding the rotor windings from the supply is shown in Fig. 2. The voltage equations can be written as (2) and (3).

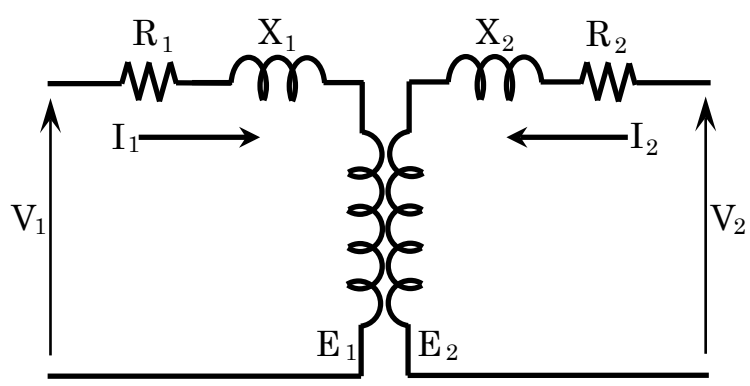

Fig. 2. The equivalent circuit per phase of DFIM.
Source: Authors.

$$V_1 = I_1 (R_1 + jX_1) + E_1 \tag{2}$$

$$V_2 = I_2 (R_2 + jX_2) + E_2 \tag{3}$$

Where V_1 is the stator input voltage per phase, V_2 is the rotor injected voltage per phase, E_1 is the induced EMF at the stator windings per phase and E_2 is the induced EMF at the rotor windings per phase. I_1 is the stator phase current and I_2 is the rotor phase current. R_1 is the stator phase resistance, R_2 is the rotor phase resistance, X_1 is the stator phase leakage reactance and X_2 is the rotor phase leakage reactance.

The input power to the stator (P_1) and the input power to the rotor (P_2) can be determined with (4), (5):

$$P_1 = 3V_1 I_1 \cos\varphi_1 \quad (4)$$

$$P_2 = 3V_2 I_2 \cos\varphi_2 \quad (5)$$

Where $cos\varphi_1$ is the power factor at the stator side and $cos\varphi_2$ is the power factor at the rotor side.

By neglecting the iron loss, the total losses can be calculated as (6), (7), (8):

$$P_{loss} = P_{c1} + P_{c2} \quad (6)$$

$$P_{c1} = 3{I_1}^2 R_1 \quad (7)$$

$$P_{c2} = 3{I_2}^2 R_2 \quad (8)$$

Where P_{C1} is the stator copper loss and P_{C2} is the rotor copper loss.

Accordingly, the DFIM mechanical power (P_m) and developed torque (T) become (9), (10):

$$P_m = P_1 + P_2 - P_{loss} \quad (9)$$

$$T = P_m/\omega \quad (10)$$

Where ω is the motor speed in (rad/s).

IV. Theoretical Results and Discussion

The performance of DFIM is tested for different conditions via Matlab Simulink depending on the mathematical model. The results are evaluated for three cases at steady state operation as follows:

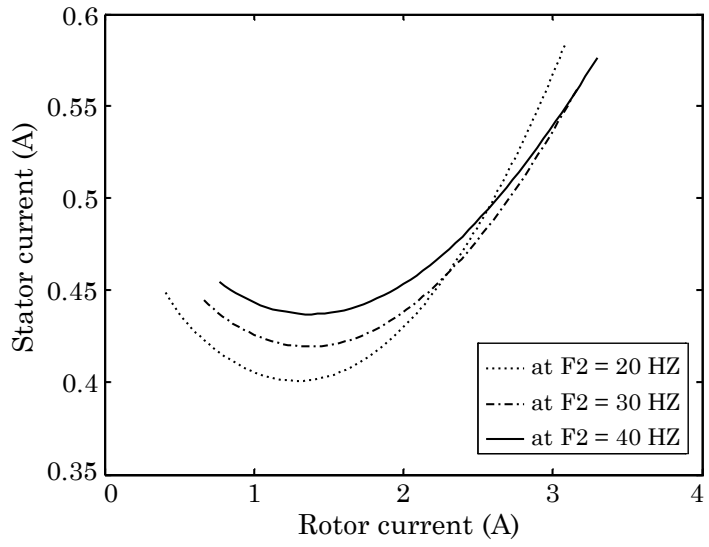

Fig. 3. Stator current versus rotor current considering different rotor frequencies at (V_1 = 210 V).
Source: Authors.

Firstly, stator voltage is constant and equal to 210 v and different rotor frequencies (F_2 = 40, 20, and 30 Hz). The stator current variation via rotor current variation is demonstrated in Fig. 3 for mentioned rotor frequencies. Clearly, the DFIM behavior is similar to the operation of a synchronous motor, and an increase in rotor frequency results in an increase in stator current.

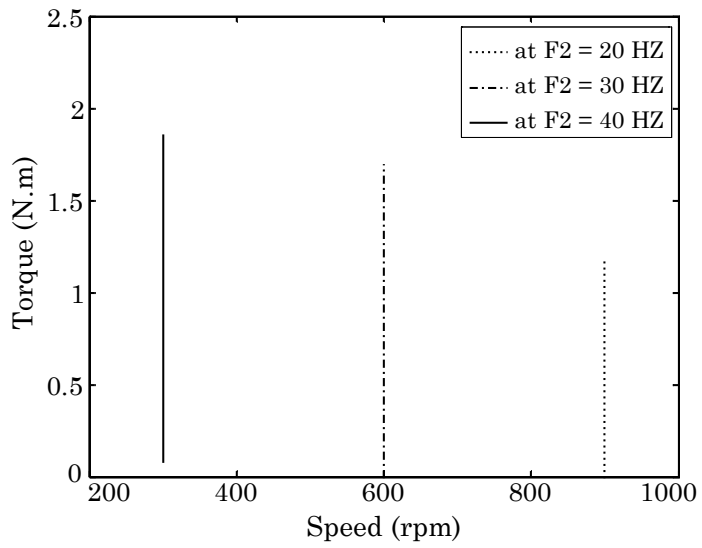

Fig. 4. Torque- speed characteristics of DFIM at different rotor frequencies at (V_1 = 210 V).
Source: Authors.

Fig. 4 displays the torque–speed characteristics for DFIM at different rotor frequency. The motor speed is fixed during torque variation; in contrast, it changes with the rotor frequency. Consequently, the motor speed and rotor frequency are in synchronism. Therefore, at steady state, the DFIM produces a synchronous torque.

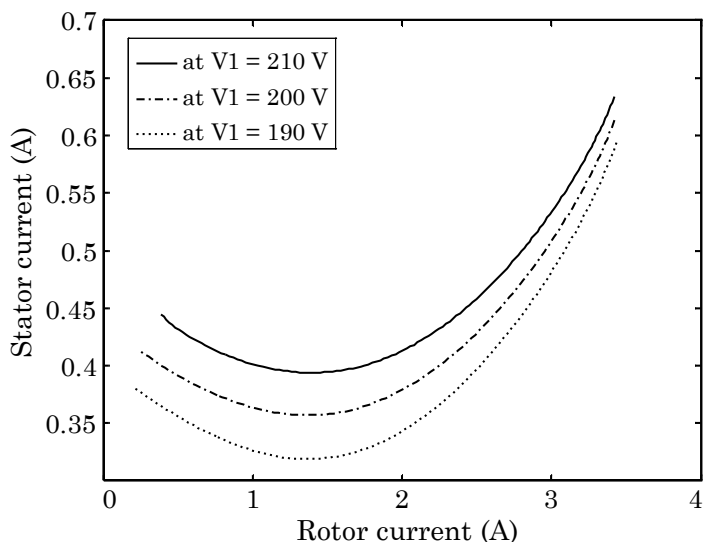

Fig. 5. Stator current versus rotor current considering different stator voltages at (F_2 = 15 Hz).
Source: Authors.

Secondly, this condition is tested at a constant frequency in the rotor equals 15 Hz and a variation in stator voltage. Stator current variation via rotor current for different stator voltage levels is illustrated in Fig. 5. The (V-curves) of DFIM varies similar to synchronous motor (V-curves). Typically, the stator voltage raises leading to increasing in stator current.

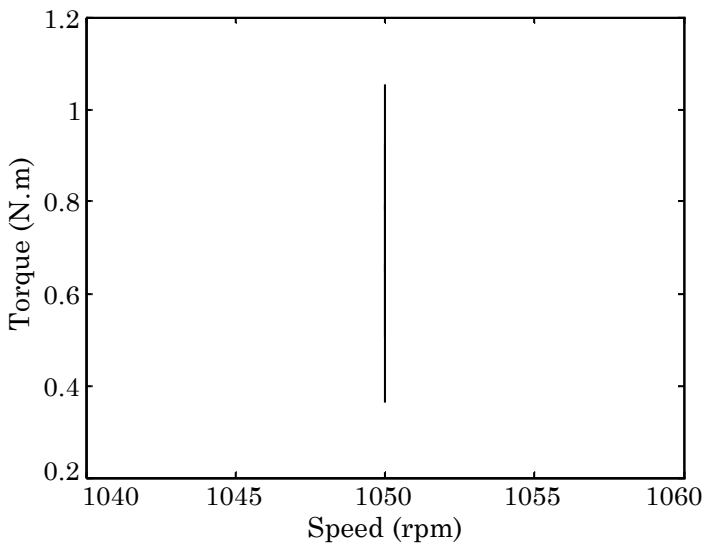

Fig. 6. Torque- speed curve of DFIM at different stator voltages at (F_2 = 15 Hz).
Source: Authors.

Fig. 6 depicts the torque–speed curves at different values of voltage in the stator. The motor speed remains constant with stator voltage variation

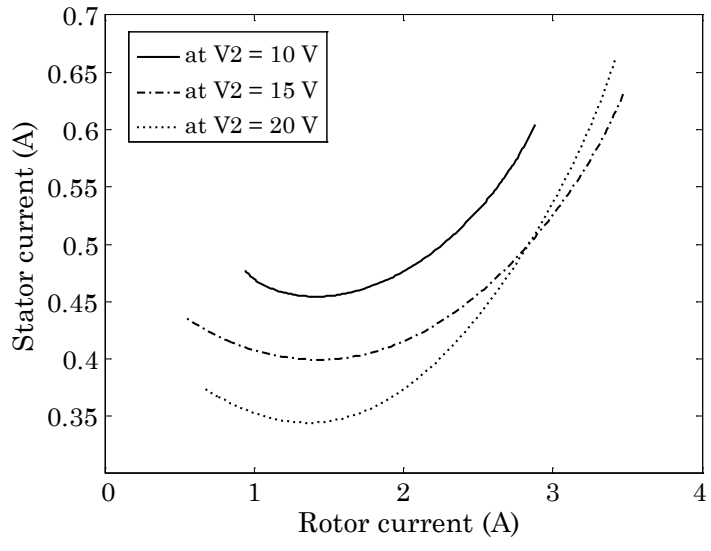

Fig. 7. Stator current versus rotor current considering different rotor voltages at (V_1 = 210V, F_2 = 15 Hz).
Source: Authors.

The motor characteristics investigated at rotor voltage variation for constant rotor frequency and stator voltage. The values of rotor frequency and stator voltage are 15 Hz and 210, respectively. For different rotor voltage levels, the variation in stator current via rotor current adopts the behaviour of (V-curves) as cleared in Fig. 7. It is noticed that that the rotor voltage and stator current are inversely related. Moreover, rotor voltage has no impact on the torque–speed curve, as evidenced in Fig. 8.

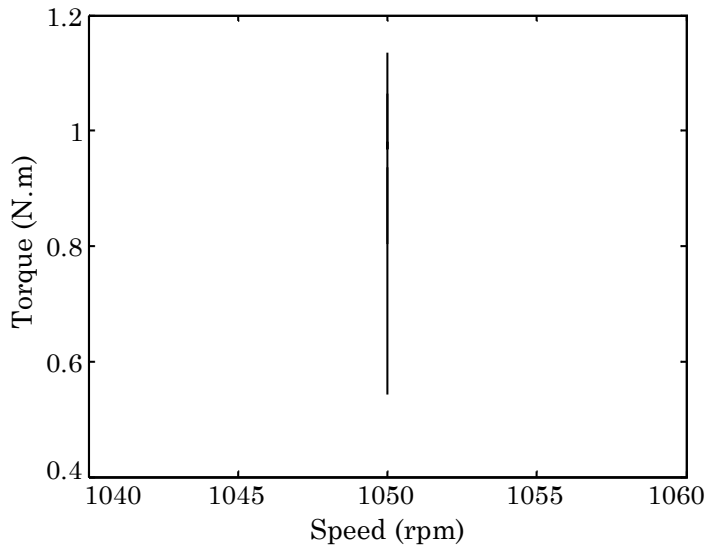

Fig. 8. Torque-speed curve of DFIM at different rotor voltages at (V_1 = 210V, F_2 = 15 Hz).
Source: Authors.

V. Experimental Setup and Results

An experimental prototype for the DFIM drive system has been built in the laboratory to verify theoretical results. According to Fig. 9, the setup mainly consists of the motor under test (DFIM) of rating (0.3kw, 230/400V, 2.2A ,1395 rpm), a DC generator as a mechanical load, a three phase transformer connected in the rotor side, and a variable frequency converter for controlling the motor speed. The setup is also composed of two three-phase auto transformers. One of them is employed between the grid side and the stator, while the other is employed between the grid and the rotor. This is done to regulate the strength of the stator and rotor voltages. All these components are labeled in the Fig. 9 and listed in Table 1.

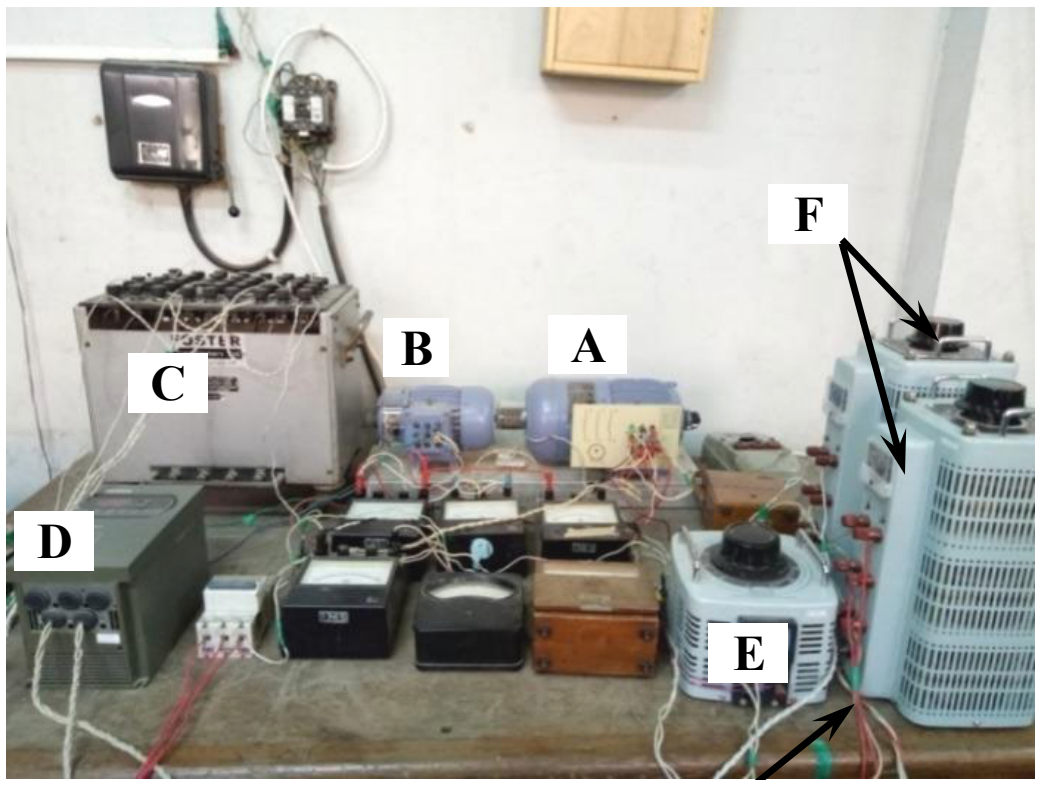

Fig. 9. Main parts of DFIM experimental setup.
Source: Authors.

TABLE 1.
COMPONENTS OF EXPERIMENTAL SETUP.

Label	Component
A	DFIM.
B	DC generator.
C	3-phase transformer.
D	Variable frequency converter.
E	1-phase auto transformer.
F	Two 3-phase auto transformers.

Source: Authors.

The experimental results are investigated for four conditions as follows.

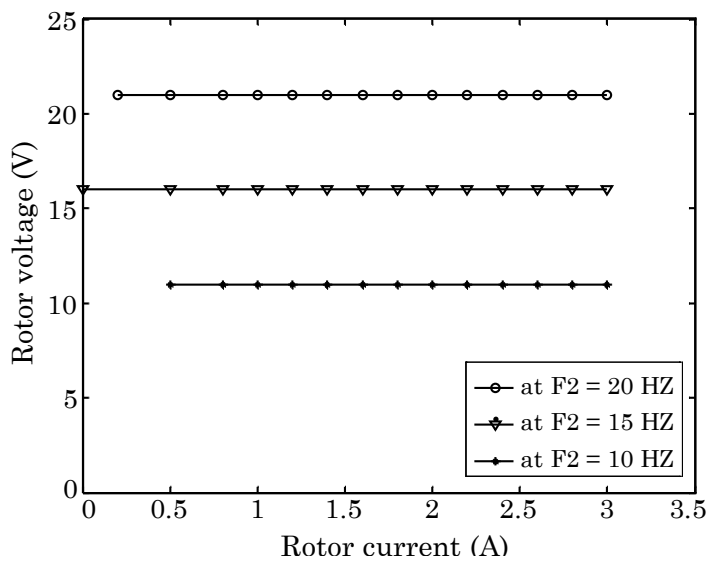

Fig. 10. Rotor voltage with rotor current at different rotor frequencies and (V_1 = 210 V).
Source: Authors.

The *first condition* is recorded at various rotor frequencies of 10 Hz, 15 Hz, and 20 Hz and a 210 V stator voltage. The variation in rotor current and stator current for rotor frequencies is displayed in Fig. 10. It is noticed that the rotor voltage remains constant with the rotor current change. However, according to the ratio (V_2/F_2 = constant), rotor voltage change is proportional to the rotor frequency.

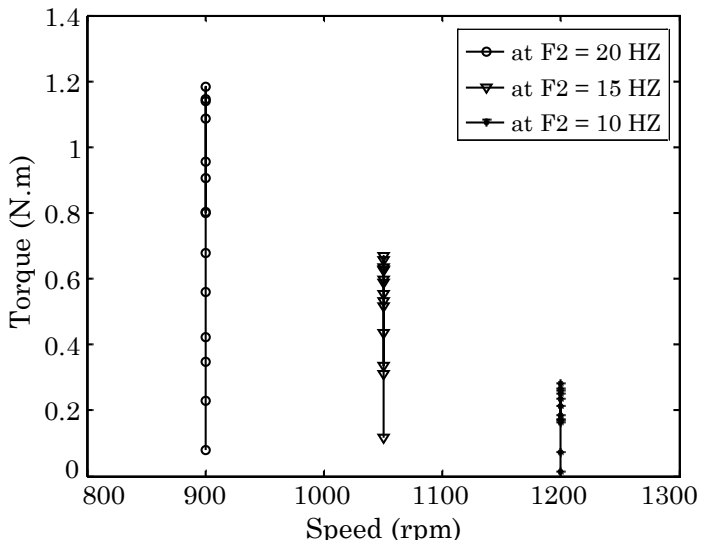

Fig. 11. Torque- speed curves of DFIM at different rotor frequencies and (V_1 = 210 V).
Source: Authors.

Furthermore, the motor speed is fixed at load torque and changes with the rotor frequency as shown in Fig. 11. This demonstrates that the DFIM has similar torque-speed characteristics of synchronous motor. The variation in stator current with rotor current, at various rotor frequencies, is recorded as illustrated in Fig. 12.

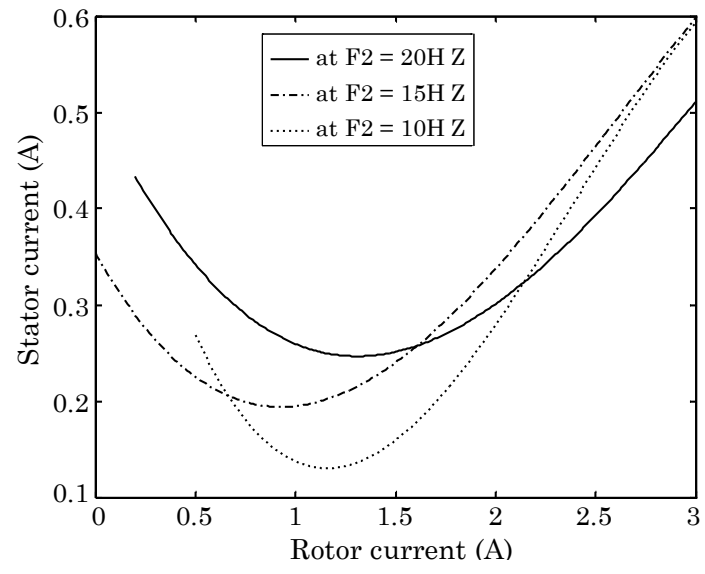

Fig. 12. Stator current with rotor current at different rotor frequencies and (V_1 = 210 V).
Source: Authors.

The *second condition* is examined the stator voltage variation on the motor characteristics. This condition is recorded for a specific rotor frequency of 15 Hz and different values of stator voltage. Additionally, the motor speed is constant at 1050 rpm, which corresponds to the rotor frequency (F_2 = 15 Hz), and is unaffected by variations in the stator voltage or load torque (Fig. 13).

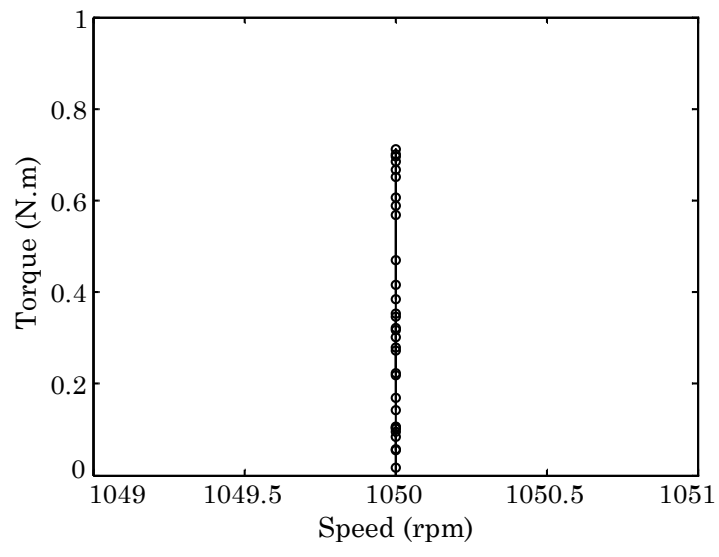

Fig. 13. Torque- speed curve of DFIM at different values of stator voltage and at (F_2 = 15 Hz).
Source: Authors.

In other words, at various values of stator voltage, the stator current varies with the rotor current in the form of (V-curves), as shown by Fig. 14. Whenever the rotor current is low, the stator current is observed to decrease by reducing the stator voltage, however as the rotor current increases. The stator current curves are converging.

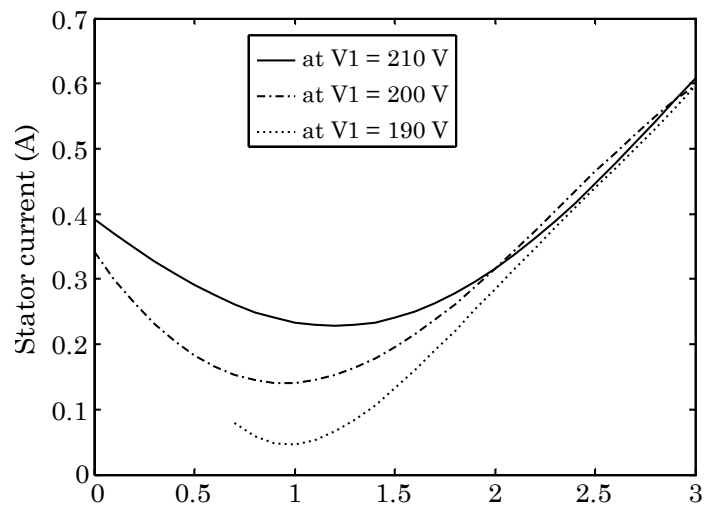

Fig. 14. Stator current versus rotor current considering different stator voltage and at (F_2 = 15 Hz).
Source: Authors.

For *third* operating point of results investigates the influence of rotor voltage variation on the motor characteristics at a fixed stator voltage and rotor frequency (V_1 = 210 V), (F_2 = 15 Hz). Despite of the variation in torque and rotor voltage, motor speed is still constant equals (1050 rpm) which correlates directly to rotor frequency (F_2 = 15 Hz), as displayed in Fig. 15.

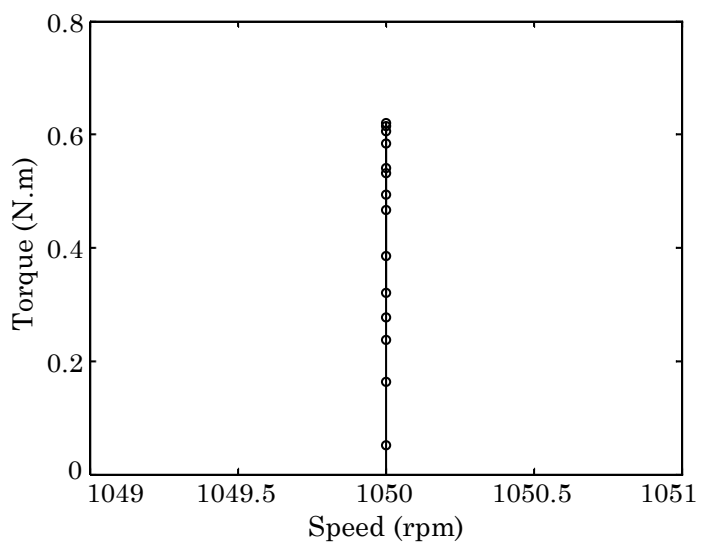

Fig. 15. Torque- speed curve of DFIM at different values of rotor voltage and at (V_1 = 210V, F_2 = 15 Hz).
Source: Authors.

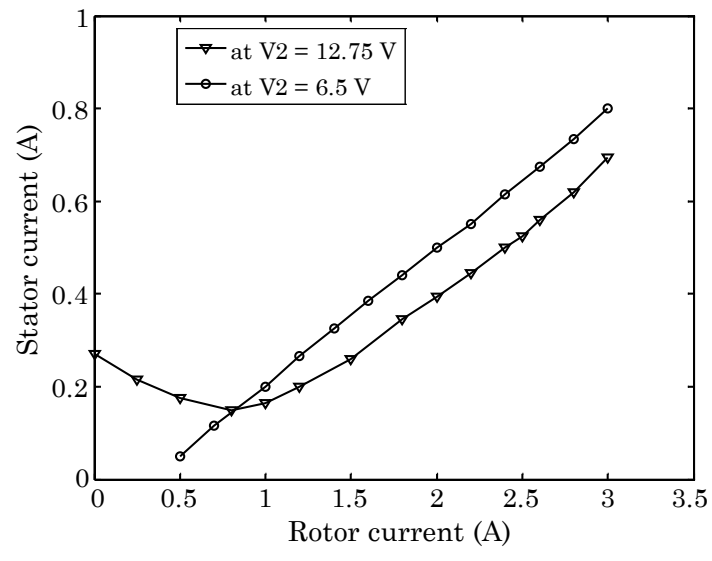

Fig. 16. Stator current versus rotor current considering different rotor voltage and at (V_1 = 210V, F_2 = 15 Hz).
Source: Authors.

According to Fig. 16, the stator current increases with the rotor current throughout the rotor voltage changes. The stator current is seen to increase throughout a wide variety range for rotor current when rotor voltage is decreased.

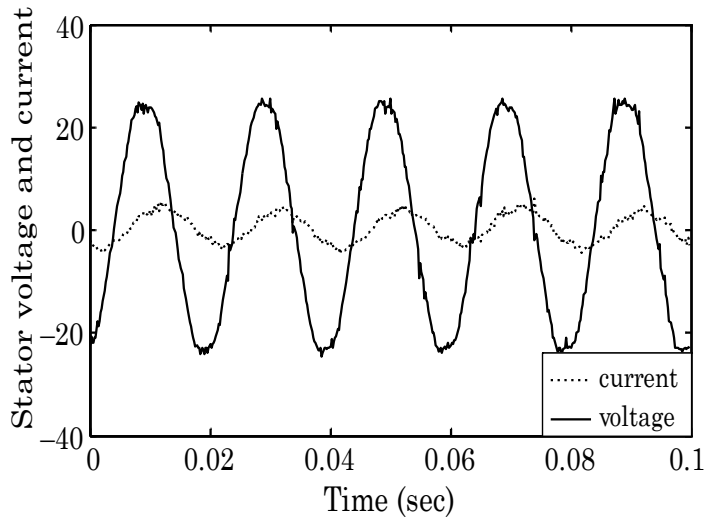

Fig. 17. Waveforms of stator phase voltage and current of DFIM at (I_2 = 0.8 A).
Source: Authors.

Finally, the impact of modifying rotor current on DFIM's power factor are discussed. For various levels of rotor current, the stator current and voltage with rotor current equals 0.8 A are recorded at (F_2 = 15 Hz and V_1 = 180 V). The Fig. 17 illustrates the output waveforms for stator phase voltage and current with rotor current equals 0.8 A. Stator current appears to be lag the phase voltage. By raising the rotor current to 1.5 A, the current and voltage are in phase and the power factor is nearly unity, as demonstrated by Fig. 18.

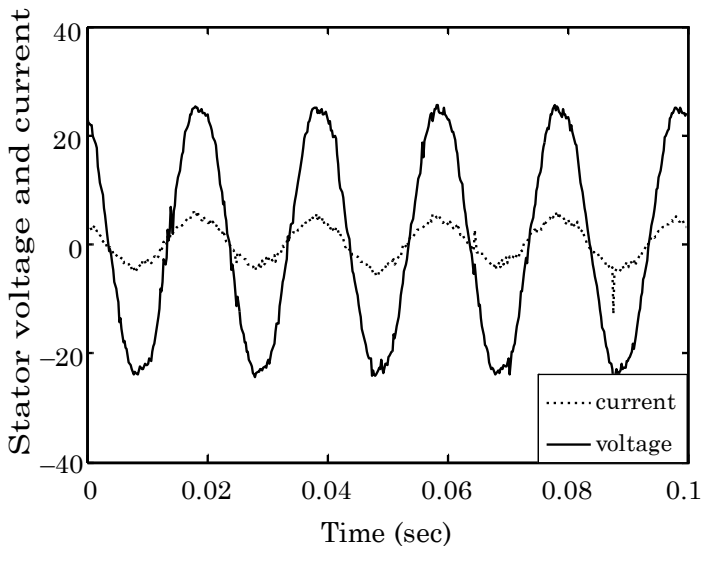

Fig. 18. Waveforms of stator phase voltage and current of DFIM at (I_2 = 1.5 A).
Source: Authors.

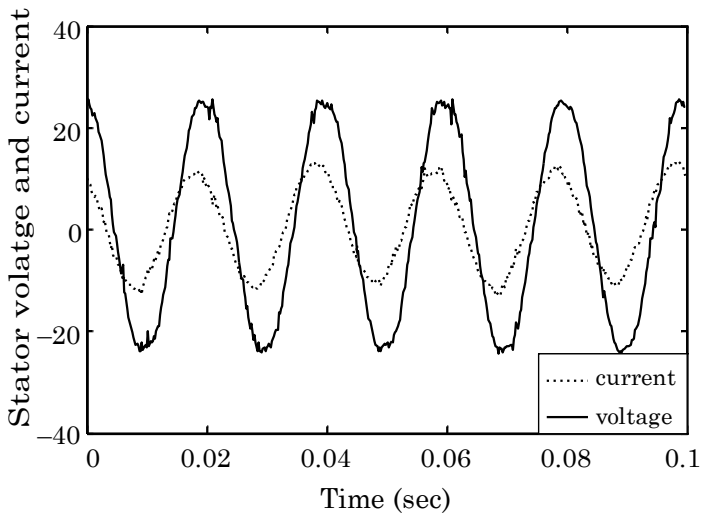

Fig. 19. Waveforms of stator phase voltage and current of DFIM at (I_2 = 2.8 A).
Source: Authors.

Continually raising in rotor current until a certain value of 2.8 A, achieves a leading power factor as evident by Fig. 19. Previous figures, the voltage multiplied by a factor of 10, and the current divided by a factor of 50. The DFIM's ability to change its power factor by adjusting the rotor current improves its performance as a synchronous motor.

VI. Conclusions

The performance evaluation for DFIM is presented in this paper. Theoretical and experimental studies are carried on during speed and load variation. The results reveal that the behavior of DFIM similar to that of synchronous motor and has the same performance characteristics. The motor speed is constant despite of variation in load torque and can only be altered by changing the rotor frequency. Both the stator voltage and rotor voltage variation have no impact on the motor speed. Eventually, the achievement of a respectable degree of agreement between theoretical and experimental focuses on the validity of the mathematical approach. Overall, the use of the DFIM in smart irrigation systems can lead to improved performance and efficiency, better control, and lower costs.

Acknowledgement

The authors extend their appreciation to the Deputyship for Research& Innovation, Ministry of Education in Saudi Arabia for funding this research work through the project number ISP22-43.

References

[1] M. Etemadi, H. Hesar & M. Khoshhava, "Speed Control of Brushless Doubly Fed Induction Machine Drive Based on Model Reference Adaptive System," presented at *13th Power Electronics, Drive Systems, and Technologies Conference*, PEDSTC, THR, IR, 1-3 Feb. 2022. https://doi.org/10.1109/PEDSTC53976.2022.9767330

[2] Y. Zhang, J. Ge, W. Xu, W. Li, Y. Luo, S. Su, & Y. He, "Performance Analysis of Nested-loop Secondary Linear Doubly-fed Machine Considering End Effects," *CES Trans Electr Mach Syst*, vol. 6, no. 3, pp. 298–305, Sept. 2022. https://doi.org/10.30941/CESTEMS.2022.00040

[3] Z. Cheng, Z. Cao, J. Hwang & C. Mi, "A Novel Single-Turn Permanent Magnet Synchronous Machine for Electric Aircraft," *Energies*, vol. 16, no. 3, pp. 1–14, Jan. 2023. https://doi.org/10.3390/en16031041

[4] N. El Ouanjli, A. Derouich, A. El Ghzizal, J. Bouchnaif, Y. El Mourabit, M. Taoussi & B. Bossoufi, "Real-time implementation in dSPACE of DTC-backstepping for a doubly fed induction motor," *Eur. Phys. J. Plus*, vol. 134, no. 11, pp. 1–14, Aug. 2019. https://doi.org/10.1140/epjp/i2019-12961-x

[5] R. Yang, Z. He, N. Sugita & T. Shinshi, "Low-Cost and Compact Disposable Extracorporeal Centrifugal Blood Pump Utilizing a Homopolar Bearingless Switched Reluctance Slice Motor," *IEEE Access*, vol. 11, pp. 24353–24366, Mar. 2023. https://doi.org/10.1109/ACCESS.2023.3254546

[6] D. Li, G. Gong, J. Lv, X. Jiang & R. He, "An Overall Control of Doubly fed Variable Speed Pumped Storage Unit in Pumping Mode," presented at *IEEE 4th Conference on Energy Internet and Energy System Integration*, EI2, WHN, CN, 30 Oct. 2020 - 1 Nov. 2020. https://doi.org/10.1109/EI250167.2020.9346705

[7] R. Selvaraj, T. Chelliah & K. Desingu, "Reactive Power Circulation Based Fault Tolerance Schemes for Multi-Megawatt 3L-NPC Paralleled Converters in Variable Speed Hydro Applications," *IEEE Trans Ind Appl*, vol. 59, no. 2, pp. 1923–1934, Mar. 2023. https://doi.org/10.1109/TIA.2022.3222647

[8] R. Mehrjardi, N. Ershad, B. Rahrovi & M. Ehsani, "Brushless Doubly-Fed Induction Machine with Feed-Forward Torque Compensation Control," presented at *IEEE Texas Power and Energy Conference*, TPEC, CS, TX, USA, 2-5 Feb. 2021. https://doi.org/10.1109/TPEC51183.2021.9384974

[9] W. Rajan Babu, M. Sundaram, G. Muthuram, A. Khaja Najumudeen, M. Karthick & B. Chandramouli, "MSCP based Rotor Faults and Mechanical Bearing Failure Identification in Induction Motor using Power Quality Analyzer," presented at *International Conference on Intelligent Data Communication Technologies and Internet of Things*, IDCIoT, BGLU, IN, 5-7 Jan. 2023. https://doi.org/10.1109/IDCIoT56793.2023.10053456

[10] M. Yahiaoui, M. Kinnaert & J. Gyselinck, "Sensorless Vector Control for Grid Synchronization of Doubly-Fed Induction Generators," presented at *International Conference on Electrical Machines*, ICEM, VAL, ES, 5-8 Sept. 2022. https://doi.org/10.1109/ICEM51905.2022.9910913

[11] C. Djamila, M. Yahia & M. Mohamed, "Performances of Robust Control of Doubly-Fed Induction Generator for Wind Energy Conversion System," presented at *2nd International Conference on Innovative Research in Applied Science, Engineering and Technology*, IRASET, MKS, MOR, 3-4 Mar. 2022. https://doi.org/10.1109/IRASET52964.2022.9737917

[12] R. Ryndzionek, K. Blecharz, F. Kutt, M. Michna & G. Kostro, "Fault-Tolerant Performance of the Novel Five-Phase Doubly-Fed Induction Generator," *IEEE Access*, vol. 10, pp. 59350–59358, May. 2022. https://doi.org/10.1109/ACCESS.2022.3179815

[13] S. Abdi, E. Abdi & H. Toshani, "Rotational Iron Losses in Brushless Doubly Fed Machines," presented at *International Conference on Electrical Machines*, ICEM, VAL, ES, 5-8 Sept. 2022. https://doi.org/10.1109/ICEM51905.2022.9910940

[14] B. Battulga, M. Shaikh, S. Bin Lee & M. Osama, "Automated Detection of Failures in Doubly-Fed Induction Generators for Wind Turbine Applications," presented at *IEEE Energy Conversion Congress and Exposition*, ECCE, DET, MI, USA, 9-13 Oct. 2022. https://doi.org/10.1109/ECCE50734.2022.9947734

[15] M. Cheng, X. Yan & J. Zhou, "Negative-Sequence Current Compensation-Based Coordinated Control Strategy for Dual-Cage-Rotor Brushless Doubly Fed Induction Generator Under Unbalanced Grid Conditions," *IEEE Trans Ind Electron*, vol. 70, no. 5, pp. 4762–4773, May. 2023. https://doi.org/10.1109/TIE.2022.3186317

[16] F. Deylami & A. Darabi, "A Simple Method for Steady-State Performance Optimization of Doubly-Fed Induction Machines," presented at *9th Iranian Conference on Renewable Energy & Distributed Generation*, ICREDG, MSHD, IR, 23-24 Feb. 2022. https://doi.org/10.1109/ICREDG54199.2022.9804516

[17] M. Mehta & B. Mehta, "Implementation of STATCOM in a Doubly Fed Induction Machine Based Wind Park," presented at *IEEE International Power and Renewable Energy Conference*, IPRECON, KLLM, IN, 16-18 Dec. 2022. https://doi.org/10.1109/IPRECON55716.2022.10059544

[18] S. Odhano, S. Rubino, M. Tang, P. Zanchetta & R. Bojoi, "Stator Current-Sensorless-Modulated Model Predictive Direct Power Control of a DFIM With Magnetizing Characteristic Identification," *IEEE J Emerg Sel Top Power Electron*, vol. 9, no. 3, pp. 2797–2806, Jun. 2021. https://doi.org/10.1109/JESTPE.2020.3024679

[19] B. Dahhou & A. Bouraiou, "Speed Control Of DFIM Using Artificial Neural Network Controller," presented at *2nd International Conference on Advanced Electrical Engineering*, ICAEE, COST, AG, 29-31 Oct. 2022. https://doi.org/10.1109/ICAEE53772.2022.9961983

[20] L. Simon, J. Ravishankar & S. Swarup, "Coordinated reactive power and crow bar control for DFIG-based wind turbines for power oscillation damping," *Wind Eng*, vol. 43, no. 2, pp. 95–113, Jul. 2018. https://doi.org/10.1177/0309524X18780385

Emad Hassan. Jazan University (Jizan, Saudi Arabia).